Available online at www.sciencedirect.com
ScienceDirect
Journal of Colloid and Interface Science 315 (2007) 248–254
JOURNAL OF Colloid and Interface Science
www.elsevier.com/locate/jcis

Quartz resonator signatures under Newtonian liquid loading for initial instrument check

Nam-Joon Cho [a,b], J. Nelson D'Amour [b], Johan Stalgren [b], Wolfgang Knoll [c], Kay Kanazawa [b], Curtis W. Frank [b,*]

[a] *Department of Materials Science and Engineering, Stanford University, Stanford, CA 94305, USA*
[b] *Department of Chemical Engineering, Stanford University, Stanford, CA 94305, USA*
[c] *Max-Planck-Institut für Polymerforschung, Ackermannweg 10, Mainz 55128, Germany*

Received 10 March 2007; accepted 13 June 2007

Available online 13 August 2007

Abstract

The quartz crystal microbalance (QCM) has been increasingly utilized in the monitoring of the deposition of thin macromolecular films. Studies in the deposition of polymers, biomaterials, and interfacial reactions under electrochemical environment are some of the conditions for the study of these material and deposition properties at a lipid interface. Numerous studies have shown the difficulties in configuring an experimental setup for the QCM such that the recorded data reflect only the behavior of the quartz crystal and its load, and not some artifact. Such artifacts for use in liquids include mounting stress, surface properties such as hydrophobicity, surface roughness coupling to loading liquids, influence of compressional waves, and even problems with the electronic circuitry including the neglect of the quartz capacitance and the hysteretic effects of electronic components. It is thought useful to obtain a simple test by which the user could make a quick initial assessment of the instrument's performance. When a smooth quartz crystal resonator is immersed from air into a Newtonian liquid, the resonance and loss characteristics of the QCM are changed. A minimum of two experimental parameters is needed to characterize these changes. One of the changes is that of the resonant frequency. The second is characterized by either a change in the equivalent circuit resistance (ΔR) or a change in the resonance dissipation (ΔD). Two combinations of these observables, in terms of either Δf and ΔR or Δf and ΔD, which we define as Newtonian signatures of S_1 and S_2, are calculated to have fixed values and to be independent of the harmonic and of the physical values of the Newtonian liquid. We have experimentally determined the values of S_1 and S_2 using three different QCM systems. These are the standard oscillator, the network analyzer, and the QCM dissipation instrument. To test the sensitivity of these signatures to surface roughness, which is potential experimental artifact, we determined the values of S_1 and S_2 for roughened crystals and found that these signatures do reflect that experimental condition. Moreover, these results were qualitatively in accord with the roughness scaling factor described by Martin.

Keywords: Quartz crystal microbalance (QCM); Newtonian liquid; Newtonian signatures; Atomic force microscope (AFM)

1. Introduction

The quartz crystal microbalance (QCM) is a sensitive technique that responds to a variety of different physical loads in contact with its surface. Changes in the quartz crystal's resonant frequency and energy loss (measured by dissipation or resistance changes) give insight as to the type and magnitude of loading. Given the flexibility of the QCM, an increasing number of applications for the QCM involve investigations of adsorption/desorption processes, deposition/dissolution of surface films, electrochemical reactions, viscoelastic film properties, and interfacial slip [1–13]. The fluids in most experimental situations are Newtonian, for which the elastic modulus is zero and the viscosity is frequency independent. A Newtonian liquid is described simply by its density, ρ_L, and its viscosity, η_L. Under this condition, the effects of the liquid can be treated as a constant offset, and the additional influences of further light loading by deposition, for example, can be treated independently [11,14]. However, researchers often find difficulty interpreting their observations of complex systems in terms of

* Corresponding author.
E-mail address: curt.frank@stanford.edu (C.W. Frank).

0021-9797/$ – see front matter
doi:10.1016/j.jcis.2007.06.020

meaningful physical properties. Naturally, questions arise as to the accuracy of the instrumentation and technique resulting from unintentional interactions at the QCM probing interface such as stress effects, temperature effects, surface roughness, and other artifacts. In order to be able to make use of the high resolution of QCM measurements, standard signatures available from standard measurements would be useful for testing the proper operation of the instrument.

In this paper, we present two such parameters that can be used to assess proper QCM instrument performance. These expressions, when applied to a smooth quartz resonator immersed in a Newtonian fluid, are constant, independent of the liquid density and viscosity, as well as the harmonic of operation. These signatures, denoted S_1 and S_2, are both derived from the analytic descriptions for the QCM provided by Martin et al. [8]. These follow the prior indications of such parameters suggested by Krim and Widom [15]. They showed that from a simultaneous measurement of quality factor and frequency shift on adsorption of a film, a film slip time can be evaluated and the interfacial viscosity of the film determined. Similarly, Lucklum et al. [16] showed the importance of the simultaneous determination of the quality factor (as measured by the equivalent resistance) and the frequency shift, which could specifically lead to a description of the imaginary and real parts of the acoustic load impedance. Also, the work of Rodahl, Kasemo, and coworkers [6,17] predates this study and, in fact, our results for S_2 can be obtained directly from their papers. It is our purpose here to provide the user who is working with a QCM instrument that records either the frequency change, Δf, and the equivalent loss resistance change, ΔR, or the frequency change, Δf, and the dissipation, D, succinct expressions by which these values can be used to provide an initial check on the proper operation of that instrument. In this paper, we show the use of these signatures in the three common methods for QCM measurements and illustrate how physical changes, such as surface roughness of the quartz resonator, can dramatically affect these values.

2. Experimental

2.1. Materials

The AT-cut quartz crystals (Maxtek) had a fundamental resonance of 5 MHz. The measured RMS roughness for the smooth crystal was 2 ± 0.5 nm. These crystals were used for the standard tests of the signature values. The water solutions were prepared in 400 ml beakers and stored under ambient conditions. To estimate the sensitivity to surface roughness, crystals having two different surface roughnesses, 300 ± 50 and 600 ± 50 nm, respectively, were used. These will be called the intermediate and rough surfaces. A 18.2 MΩ cm of Milli-Q water (MilliPore) was used for all experiments.

2.2. Instruments

In this work, we used three different instruments to measure the influence of surface roughness. The first one was the Research Quartz Crystal Microbalance (RQCM, Maxtek), which measures frequency and resistance changes at the fundamental resonance. The second was the Quartz Crystal Microbalance with Dissipation (QCM-D, Q Sense), which was used to measure the changes in frequency and dissipation at four harmonics, both simultaneously and continuously. We also used a network analyzer (E5100A, Hewlett–Packard) to measure the full impedance spectrum at four harmonics. In the impedance analysis method, the loss can be characterized by either the Q (ratio of the resonant frequency to the full width at half-maximum) and/or by the resistance (maximum conductance). Either or both D and R may be obtained. To accommodate the possibility of using D and/or R to characterize the loss, we obtain two signatures, one involving Δf and ΔR and another involving Δf and ΔD. All quartz crystals were mounted in Kynar probe holders (Maxtek). The use of the Kynar probe holder was effective in minimizing any unintentional coupling between the crystal electrode and the liquid. Specifically, the larger electrode was used to directly interface to the liquid and its electrical potential was zero. The Kynar probe also ensures a large distance between the smaller excited electrode and the liquid. The effective capacitive coupling then between the excited electrode and the liquid was minimal. In addition, the crystal was immersed with its face vertical rather than horizontal, minimizing the effects of the compressional waves. The physical roughness of the quartz crystals (intermediate and rough) was measured using an Alpha-Step 200 profilometer (Tencor Instruments; estimated precision of 50 nm) provided by Maxtek. Topographic atomic force microscope (AFM) images were measured on a XE-100 (PSIA Sungnam) in contact mode with Si_3N_4 cantilevers (Veeco). The RMS roughness values for all three surfaces derived from the AFM images were comparable to the profilometer results.

2.3. Methods

Each quartz crystal was oxygen-plasma-cleaned (March Plasmod Plasma Etcher) at 75 W for 5 min prior to measurements in order to remove organics and render the surface hydrophilic.

Different measurement procedures were followed for each instrument.

2.3.1. RQCM

After the crystal was mounted, a baseline in air was taken for at least 10 min. Prior to data collection, the stray capacitance was compensated by manually adjusting two capacitor plates on the oscillator. This ensured precise values of the resistance. The crystal was then placed into a beaker filled with water and allowed to stabilize to minimize changes in the effects of stress and pressure, meanwhile canceling the stray capacitance again (by minimizing the measured resistance).

2.3.2. QCM-D

Stray capacitance does not affect the measurement with the QCM-D since the crystal is short-circuited after being driven at the resonant frequency. The decaying waveform is subsequently analyzed to obtain the experimental observables of frequency

and dissipation. To collect the unloaded baseline, the resonant frequencies at each of the four harmonics were first determined and then monitored until stable. The measurement was then halted and the probe was placed in the liquid. We searched again for the resonant frequencies and continued to monitor for changes until these frequencies were stable for at least 10 min.

2.3.3. Network analyzer

As the network analyzer is used for obtaining a full impedance spectrum, extra care must be taken to ensure accuracy in the measurements. Capacitance compensation is critical for high resistance measurements, especially for higher harmonics. However, it does not affect the position of the maximum conductance at the resonant frequency. Stray capacitance affects the measured resistance values causing the admittance curve to move along the vertical axis (either positive or negative). Simple three-port calibration (open, short, and 50 Ω load) does not remove this error. Through a series of tests with the holder in liquid, we determined an approximate stray capacitance of our assembly. Using extra coaxial cable, we calibrated with additional static capacitance to effectively remove the offset from the measurements. Also, it should be noted that the higher the resistance, the greater the error since the network analyzer is most accurate around its source impedance of 50 Ω. Calibration and compensation were performed for every individual measurement in air and water for each harmonic. Because of inherent circuit limitations, we did not utilize the internal circuit analysis routines for determining the equivalent circuit parameters. We acquired both the raw conductance and the susceptance traces for each measurement and fit a Lorentzian to the conductance trace to extract the resonant frequency and resistance at the maximum conductance. The bandwidth obtained from the Lorentzian curvefit was equivalent to the bandwidth derived from the inflection points on the susceptance trace. Dividing the bandwidth by the resonant frequency yields the dissipation. Custom LabVIEW programs were used to control and acquire data from the network analyzer.

2.4. Theory

A suitable depiction of quartz resonators is the electrical equivalent circuit. The Butterworth–van Dyke (BVD) circuit can represent any quartz or piezoelectric resonator with an electrostatic field source, as shown in the unloaded quartz crystal section of Fig. 1. The main advantage of the equivalent circuit model is that standard circuit analysis tools can be used to extract the equivalent circuit parameters from the electrical measurements. With the continuum electromechanical model, Martin, Granstaf, and Frye (MGF) [8] have derived equivalent circuits for the QCM resonance. Though there are other approaches to express QCM responses, we limit the discussion here to that appropriate for the QCM in liquid, and use MGF to derive the signatures.

The well-established Butterworth–van Dyke equivalent circuit has provided an excellent platform for relating electrical properties of the circuit to the mechanical properties of deposited films. As shown in Fig. 1, the equivalent circuit consists

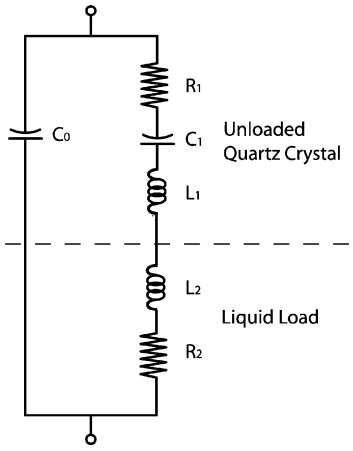

Fig. 1. The modified Butterworth–van Dyke equivalent circuit for the QCM immersed in liquid.

of two parallel branches that represent the static (C_0) and motional characteristics (L_1, C_1, R_1) of the unloaded resonator. The right-hand branch describes the quartz resonator that consists of the motional resistance, R_1, describing the losses in the crystal; the capacitance, C_1, which is analogous to an elastic modulus; and the inductance, L_1, whose inertial element is related to the displaced mass. The shunt capacitance, C_0, on the left-hand branch results from the dielectric properties of the quartz disk and interconnection capacitances [1]. Martin et al. [8] treated rigid elastic films and viscous fluids by an inductance and resistance in series and derived the modified BVD equivalent circuit (under the dashed lines).

We present here a system of annotation that delineates the harmonic frequencies studied. In the case of the fundamental resonant frequency for the in-air unloaded resonator, we write f_{1U}, where the subscript 1 represents the overtone order and the subscript U refers to the unloaded condition of the resonator.

As noted earlier, the components on the right-hand branch describe the oscillation of the quartz and its load. Indeed, it will be evident that in order to prevent errors, the value of the capacitance, C_0, on the left-hand side must be canceled out to zero. The resonant frequency of the right-hand side is given as

$$f = \frac{1}{2\pi((L_1 + L_2)C_1)^{0.5}}. \tag{1}$$

As can be seen from Eq. (1), the immersion of the QCM crystal from air to liquid results only in a change in the inductance, L_2. When $L_2 = 0$, the unloaded frequency of the fundamental is f_{1U} and, after the equation is linearized, the change in frequency becomes

$$\Delta f \cong -\frac{1}{2} f_{1U} \frac{L_2}{L_1}. \tag{2}$$

In order to express Eq. (2) such that it contains only the fundamental parameters of the unloaded quartz and the liquid parameters, we used the MGF [8] equations for C_1, L_1, and L_2:

$$C_1 = \frac{8K_0^2 \varepsilon_{22} A_M}{N^2 \pi^2 h_Q}, \tag{3}$$

$$L_1 = \frac{1}{\omega_s^2 C_1}, \tag{4}$$

Table 1
AT-cut quartz physical properties [8,24]

Description	Parameter symbol	Value
Maxtek electrode area	A_M	0.3149×10^{-4} m^2
Q-Sense electrode area	A_Q	0.2114×10^{-4} m^2
Density	ρ_Q	2650 kg/m^3
Shear modulus	c_{66}	2.901×10^{10} Pa
Piezoelectric constant	e_{26}	-0.0966 C/m^2
Permittivity	ε_{22}	3.982×10^{-11} F/m
Piezoelectrically stiffened shear modulus	$\bar{c}_{66} = c_{66} + (e_{26}^2/\varepsilon_{22})$	2.947×10^{10} Pa
Electromechanical coupling constant	$K_0 = e_{26}/\sqrt{\bar{c}_{66}\varepsilon_{22}}$	-0.0892
Thickness (for 5 MHz resonance)	h_Q	3.3170662×10^{-4} m

$$L_2 = \frac{\omega_s L_1}{N\pi}\left(\frac{2\rho_L\eta_L}{\omega\bar{c}_{66}\rho_Q}\right)^{0.5}. \tag{5}$$

All physical properties of the AT-cut quartz crystal are defined and summarized in Table 1.

Taking Nf_{1U} for the unloaded Nth harmonic resonant frequency, f_{NU}, we find the resulting frequency change on immersion into the liquid to be

$$\Delta f = -N^{0.5} f_{1U}^{3/2}\left(\frac{\rho_L\eta_L}{\pi\rho_Q\bar{c}_{66}}\right)^{0.5}. \tag{6}$$

Taking the MGF equation for resistance, we derive a comparable expression for the resistance changes after the QCM crystal is changed from air to liquid loading:

$$R_2 = \frac{\omega_s L_1}{N\pi}\left(\frac{2\omega\rho_L\eta_L}{\bar{c}_{66}\rho_Q}\right)^{0.5}. \tag{7}$$

Since the frequency change during immersion is negligible compared to the unloaded resonant frequency, we set the resonant frequency ω equal to the resonant frequency ω_s measured in air, and express the resistance change as

$$\Delta R = R_2 = \frac{\pi\bar{c}_{66}h_Q}{8e_{26}^2A_M}\left(\frac{N}{f_{1U}}\right)^{0.5}\left(\frac{\rho_L\eta_L}{\pi\rho_Q\bar{c}_{66}}\right)^{0.5}. \tag{8}$$

We have expressed the resistance as a resistance change in the event that for a specific user crystal, the unloaded resistance may not be negligible. Equations (6) and (8) characterize a proportional change in resonant frequency and motional resistance occurring during contact with a Newtonian liquid. Both equations comprise the same form of quartz modulus and liquid parameters. The ratio of these changes leads to equations that are independent of both liquid parameters and the harmonic order. This ratio is designated here as the first signature, S_1:

$$S_1 = \frac{|\Delta f|}{\Delta R} = \frac{8e_{26}^2 f_{1U}^2 A_M}{\pi\bar{c}_{66}h_Q}. \tag{9}$$

The Maxtek crystal has an S_1 value of 2.03. This simple expression can be used to verify the proper operation of instruments when the Maxtek QCM crystal is immersed in a Newtonian fluid. It is independent of the fluid properties. However, it still depends on the active area of the electrode. A more preferable signature would not include an active area term, since we must measure the active area experimentally. While RQCM measurements provide resistance changes, the QCM-D measurements yield information regarding viscous loading through the dissipation parameter. Using Eq. (2) above, one can see that for the usual changes in the frequency that amount to KHz or less, the value of L_2 is negligibly small compared to L_1. The change in the dissipation caused by immersion into a liquid can then be approximated by the relation:

$$\Delta D = \frac{R_2}{\omega_{NU}L_1}. \tag{10}$$

Both the resistance, R_2, and the inductance, L_1, contain information about the active area in the same fashion. The dissipation, D, therefore, will be area independent. We can express the change in dissipation as

$$\Delta D = \left(\frac{4\rho_L\eta_L f_{1U}}{N\pi\rho_Q\bar{c}_{66}}\right)^{0.5}. \tag{11}$$

From Eqs. (6) and (11), we take the ratio of the frequency change divided by the product of the harmonic number and the dissipation change and define the second signature, S_2:

$$S_2 = \frac{|\Delta f|}{N\Delta D} = \frac{f_{1U}}{2}. \tag{12}$$

This extraordinary expression indicates that a smooth quartz resonator in air that is immersed in a Newtonian liquid turns out to have an S_2 value that is one-half the fundamental frequency of the quartz crystal. Since the fundamental frequency of a QCM crystal in air is 5.000 MHz, S_2 equals 2.5×10^6 s^{-1}. This is now independent of both the harmonic number and the active area.

Note that the change in frequency and resistance can be derived alternatively from the acoustic impedance equivalence concept [18], but we decided to develop our signatures based on the MGF work. For convenience, we derived all the expressions from this approach only, but note that the expressions could also be derived directly from results by Rodahl, Kasemo, and co-workers [6,17].

3. Results

We show the topographic AFM images of the three different surfaces in Fig. 2. From the images it is clear that the roughness is not uniform for the latter two; there exists a distribution of feature sizes. We do not take this into account in our later analysis but note how this might affect resonant frequency changes. Comparison images were taken on a SEM since the aspect ratio of the cantilever tip in AFM can skew topographic information on rough surfaces. Feature sizes from the images (not shown) were nearly equivalent for the surfaces.

Comparing the experimental data for the smooth surface with the theoretical values in Table 2, we see reasonable agreement with predicted frequency, resistance, and dissipation values. The S_1 and S_2 parameters deviate ± 3 and $\pm 8\%$ from the theoretical values, respectively. While these deviations are not negligible, we feel that they are sufficiently small to demonstrate that the instruments are working properly. From this, we

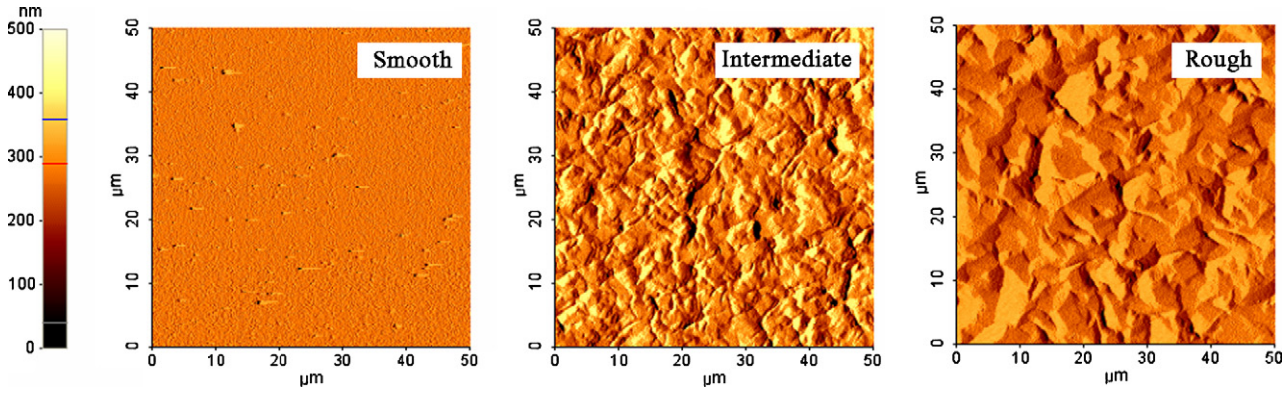

Fig. 2. Topographic contact mode of AFM images for three different surface roughnesses: smooth (2 nm), intermediate (300 nm), and rough (600 nm), where the RMS roughnesses are indicated in parentheses.

Table 2
Comparing experimental data and theoretical values using Eqs. (5)–(9) with water viscosity and density data taken from Ref. [25]

Surface	Harmonic	ΔF (Hz)	ΔR (Ω)	S_1	ΔD (1E–6)	S_2 (1E–6 s^{-1})
Smooth (0 nm)	1	−716	357	2.01	286	2.50
Theoretical values	3	−1239	618	2.00	165	2.50
	5	−1599	798	2.00	128	2.50
	7	−1892	944	2.00	108	2.50
Smooth (2 nm)	1	−714	367	1.95	310	2.30
	3	−1264	619	2.04	160	2.63
	5	−1662	827	2.01	125	2.66
	7	−1957	935	2.09	104	2.70

Table 3
RQCM results

Surface	ΔF (Hz)	ΔR (Ω)	S_1
Smooth (2 nm)	−711	351	2.03
Intermediate (300 nm)	−1099	340	3.23
Rough (600 nm)	−1595	385	4.15

estimate that deviations under 10% are acceptable for proper instrument operation.

Table 3 shows the RQCM measurements in the case of water for each surface. Since the RQCM only measures frequency and resistance, we only calculated S_1. The frequency shift increased proportionally with surface roughness. While the resistance did not change significantly in any one direction, the frequency dominated S_1 and the values increased. The values of S_1 for the intermediate and rough crystals were significantly larger than for the smooth crystal.

Table 4 shows the data obtained from the QCM-D measuring frequency and dissipation in water at four harmonics. Frequency shifts were comparable to those for the RQCM. Higher harmonics show equivalent trends as the fundamental resonance. The dissipation values also have a small, but systematic, increase with surface roughness. Hence, similar to S_1, S_2 values increase with surface roughness and increase with overtone order for the intermediate and rough surfaces.

With the network analyzer, we obtain the full admittance spectrum that can then be interpreted in terms of the equivalent circuit elements. With this complete information, we calculated

Table 4
QCM-D results

Surface	Harmonic	ΔF (Hz)	ΔD (1E–6)	S_2 (1E–6 s^{-1})
Smooth (2 nm)	1	−719	310	2.32
	3	−1259	160	2.62
	5	−1641	125	2.62
	7	−1949	105	2.64
Intermediate (300 nm)	1	−1237	329	3.76
	3	−2578	176	4.87
	5	−3794	138	5.50
	7	−4924	116	6.06
Rough (600 nm)	1	−1753	359	4.89
	3	−3954	210	6.27
	5	−5974	172	6.96
	7	−7806	147	7.60

both S_1 and S_2 for each surface. Table 5 summarizes these results. The data confirm those obtained from the two previous instruments; similar values were found for all measured parameters.

4. Brief discussion of roughness

Several models have been developed that predict the change in resonant frequency of a loaded quartz resonator as a function of surface roughness [19–22]. These reflect the additional mechanisms that arise when moving away from ideally smooth surfaces: the generation of a nonlaminar flow, pressure gradients perpendicular to the surface caused by in-plane surface motion, and the trapping of liquid by cavities and pores [20]. Theisen et al. derive an equation for the change in frequency for a surface with an average vertical deflection about the mean, h_m, for a wetting interface [19]. The equation

$$\Delta f = -\frac{f_{1U}^2 N^{0.5}}{(\rho_Q \mu_Q)^{0.5}} \left(\frac{\rho_L \eta_L}{\pi f_{1U}}\right)^{0.5} \left(1 + \frac{\pi h_m}{\lambda \delta}\right), \tag{13}$$

where $\delta = (2\eta_L/\pi f_{NU}\rho_L)^{1/2}$ is the shear wave decay length and λ is a length scaling parameter we have added, has two terms: the first is the Kanazawa description of a smooth surface and the second is the added mass contribution due to entrained liquid on the rough surface (h_m thick). The latter term is simply a Sauerbrey-like contribution. A more extensive treatment

Table 5
Network analyzer results

Surface	Harmonic	ΔF (Hz)	ΔR (Ω)	S_1	ΔD (1E–6)	S_2 (1E–6 s^{-1})
Smooth (2 nm)	1	−714	367	1.95	310	2.30
	3	−1264	619	2.04	160	2.63
	5	−1662	827	2.01	125	2.66
	7	−1957	935	2.09	104	2.70
Intermediate (300 nm)	1	−1237	340	3.64	326	3.80
	3	−2582	604	4.28	176	4.90
	5	−3817	730	5.23	138	5.55
	7	−5014	662	7.57	115	6.25
Rough (600 nm)	1	−1829	405	4.52	382	4.79
	3	−4000	735	5.44	210	6.34
	5	−6029	998	6.04	178	6.77
	7	−8087	778	10.39	160	7.22

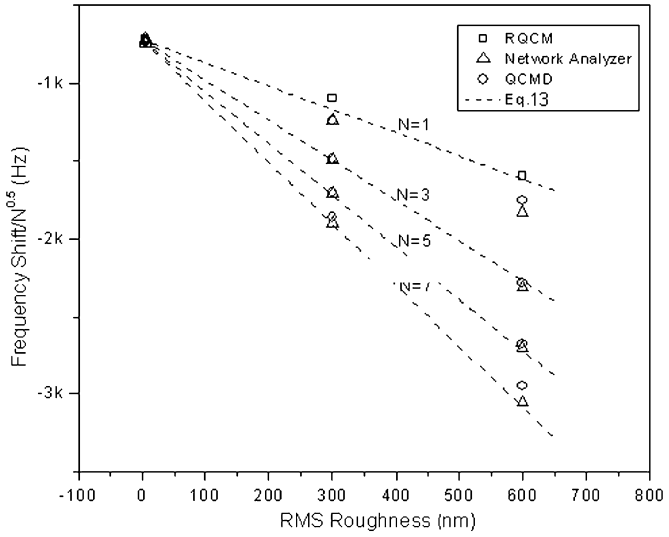

Fig. 3. Frequency shifts scaled by $N^{0.5}$ versus quartz crystal surface roughness as measured by RQCM, QCM-D, and the network analyzer. Dashed lines are predictions from Eq. (13) that incorporate a scaling parameter, λ, equal to 1/6 for all harmonics.

of surface roughness was performed by Daikhin and co-workers differentiating between slight and strong roughness along with a combination of the two [20,23]. In their strong roughness case ($h_m/\delta \geqslant 1$), they derived expressions for the frequency and bandwidth shifts in terms of an interfacial layer thickness and a local permeability term. The overall result for the frequency changes, depending on the choice of the length scaling parameter, λ. A value of $\lambda = 1/6$ fits the data better than the value $\lambda = 1$ used by Daikhin and co-workers [20,23]. However, with our limited data set, it was not possible to determine the physical significance of this length scaling parameter.

Fig. 3 shows all the harmonic data from the three instruments. Also displayed are the best fit lines to each harmonic with $\lambda = 1/6$. There is a good agreement as a function of overtone order, suggesting that the N dependence in Eq. (13) is correct. Whereas the original form of Eq. (13) used the value $\lambda = 1$, we find that the original form greatly overstates the amount of entrained water using the RMS roughness as the h_m parameter. Perhaps, this is not surprising since the underlying basis of Eq. (13) involves a periodic surface structure without varying length scales. As seen from Fig. 2, however, the length scales of the roughness vary and are randomly distributed. Still, although this value of λ is quite different from the $\lambda = 1$ postulated by Theisen et al. [19] with only a simple additional scaling constant, Eq. (13) predicts rather well the changes in frequency. It may be that as the shear wave decay length decreases with increasing overtone order, the quartz surface feels less of the fluid and probes a greater proportion of rigidly coupled fluid compared with the fundamental resonance. The fluid would then have little motion relative to the quartz interface. This agrees with the resistance and dissipation data (energy loss terms) that did not show significant changes with surface roughness at higher overtones relative to the smooth surface.

5. Conclusion

We have developed two signatures, S_1 and S_2, which can be used as indicators of proper instrument measurement under Newtonian liquid loading conditions. They are both independent of the liquid parameters and S_2 is also independent of electrode area. Using three different instruments, RQCM, QCM-D, and network analyzer (with a unique data collection procedure), we found that the values of S_1 and S_2 were in accord with predictions. Surface roughness has a large effect on QCM response under liquid loading. S_1 and S_2 values, in turn, are proportional to the degree of surface roughness with the frequency dominating the changes. Using the work of Theisen et al. [19], we analyzed the rough surfaces in terms of an entrained water layer rigidly coupled to the surface. We found that the length scale in the equation needed to be modified to account for the multiscale dimensions of the surface topography. This scaling factor, $\lambda = 1/6$, stayed constant for all harmonics. As a result, we have demonstrated the usefulness of S_1 and S_2 as a means to characterize quartz resonator systems and have identified one cause for significant deviations, surface roughness.

Acknowledgments

We thank Maxtek, Inc., for providing the custom quartz crystals, in particular John Hildebrand, Cleve Hildebrand, and Long Hoang. Also, we thank PSIA, Inc., for access to their XE-100 AFM system. This work was supported in part by NASA

1025-679-1-REDAL and the Center for Polymer Interfaces and Macromolecular Assemblies, an NSF Materials Research Science and Engineering Center.

References

[1] H.L. Bandey, S.J. Martin, R.W. Cernosek, A.R. Hillman, Anal. Chem. 71 (1999) 2205–2214.
[2] D.A. Buttry, M.D. Ward, Chem. Rev. 92 (6) (1992) 1355–1379.
[3] D. Johannsmann, J. Appl. Phys. 89 (11) (2001) 6356–6364.
[4] G. McHale, R. Lucklum, M.I. Newton, J.A. Cowen, J. Appl. Phys. 88 (12) (2000) 7304–7312.
[5] C.E. Reed, K.K. Kanazawa, J.H. Kaufman, J. Appl. Phys. 68 (5) (1990) 1993–2001.
[6] M. Rodahl, F. Hook, A. Krozer, P. Brzezinski, B. Kasemo, Rev. Sci. Instrum. 66 (7) (1995) 3924–3930.
[7] M. Yang, M. Thompson, Langmuir 9 (8) (1993) 1990–1994.
[8] S.J. Martin, V.E. Granstaff, G.C. Frye, Anal. Chem. 63 (20) (1991) 2272–2281.
[9] G.L. Hayward, M. Thompson, J. Appl. Phys. 83 (4) (1998) 2194–2201.
[10] W. Hinsberg, F.A. Houle, S.W. Lee, H. Ito, K. Kanazawa, Macromolecules 38 (5) (2005) 1882–1898.
[11] M.D. Ward, D.A. Buttry, Science 249 (4972) (1990) 1000–1007.
[12] B.Y. Du, E. Goubaidoulline, D. Johannsmann, Langmuir 20 (24) (2004) 10617–10624.
[13] F. Josse, Y. Lee, S.J. Martin, R.W. Cernosek, Anal. Chem. 70 (2) (1998) 237–247.
[14] K.K. Kanazawa, J.G. Gordon, Anal. Chem. 57 (8) (1985) 1770–1771.
[15] J. Krim, A. Widom, Phys. Rev. B 38 (17) (1988) 12184–12189.
[16] R. Lucklum, C. Behling, P. Hauptmann, Anal. Chem. 71 (13) (1999) 2488–2496.
[17] M. Rodahl, B. Kasemo, Sens. Actuat. A 54 (1–3) (1996) 448–456.
[18] B.A. Auld, Acoustic Fields and Waves in Solids, vol. 1, Wiley, New York, 1973, chap. 7.
[19] L.A. Theisen, S.J. Martin, A.R. Hillman, Anal. Chem. 76 (3) (2004) 796–804.
[20] L. Daikhin, E. Gileadi, G. Katz, V. Tsionsky, M. Urbakh, D. Zagidulin, Anal. Chem. 74 (3) (2002) 554–561.
[21] L. Daikhin, M. Urbakh, Langmuir 12 (26) (1996) 6354–6360.
[22] M. Urbakh, L. Daikhin, Phys. Rev. B 49 (7) (1994) 4866–4870.
[23] M. Urbakh, L. Daikhin, Abstr. Papers Am. Chem. Soc. 212 (1996) 82.
[24] A. Arnau, D. Soares, in: A. Arnau (Ed.), Springer-Verlag, Berlin, 2004, pp. 1–37.
[25] D.R.E. Lide, Handbook of Chemistry and Physics, CRC Press, Boca Raton, FL, 2005.